DIGITAL ROCK PHYSICS ANALYSIS OF SEISMIC PROPERTIES OF A FRACTURED SHALE FROM THE VACA MUERTA FORMATION

Simón Lissa[1,4], Nicolás D. Barbosa[1], Emilio Camilion[2], Guido Panizza[2,3], Santiago Solazzi[1], Germán Rubino[3], Beatriz Quintal[1]

1: University of Lausanne, Suiza.

2: YPF Tecnología S.A. (Y-TEC), Argentina.

3: CONICET, Argentina.

4: FCAGLP, UNLP, Argentina

Keywords: Vaca Muerta shale, seismic attenuation and velocity dispersion, fluid pressure diffusion, digital rock physics

ABSTRACT

La detección y caracterización de fracturas en rocas es relevante en la exploración y producción de hidrocarburos debido a que las fracturas representan conductos preferenciales de flujo. Dado que las ondas sísmicas son sensibles a la presencia, orientación y las propiedades de las fracturas en rocas, los métodos sísmicos pueden ser utilizados para explorar formaciones geológicas fracturadas. En rocas fracturadas y saturadas, la deformación causada por una onda incidente tiende a generar gradientes de presión y flujo de fluidos entre regiones del medio con diferentes compresibilidades. Para ciertas frecuencias y longitudes de onda incidentes mayores que el tamaño característico de la red de fracturas, las ondas sísmicas pueden experimentar alta atenuación y dispersión de la velocidad debido a la difusión de presiones de fluido. En rocas con baja permeabilidad intrínseca (por ejemplo, lutitas) y para frecuencias dentro del rango sísmico o superiores, dicho proceso ocurre principalmente entre fracturas conectadas hidráulicamente. En este estudio, aplicamos un flujo de trabajo numérico basado en imágenes tomográficas de rocas para calcular la respuesta sísmica de una muestra de lutitas fracturada perteneciente a la Formación Vaca Muerta. Los resultados muestran valores de atenuación y dispersión de la velocidad medibles en el rango de frecuencias sónicas y ultrasónicas debido a difusión de presión de fluido entre las fracturas. A continuación, estudiamos la respuesta de modelos 2D, creados a partir de una sección transversal del modelo 3D, considerando diferentes longitudes de fractura y fluidos saturantes. Finalmente, exploramos la sensibilidad sísmica a la conectividad de las fracturas.

INTRODUCTION

Oil and gas production from unconventional reservoirs has become a widespread practice in the past decade (Aguilera *et al.* 2014). In general, unconventional reservoirs consist of rocks that, due to their low permeability (e.g., shales, tight sandstones), cannot be exploited by means of conventional extraction techniques. The presence of fractures in a given geological unit significantly reduces the stiffness of the medium and greatly increases the associated permeability, as fractures are preferential fluid pathways (Zimmerman and Main 2004). For these reasons, fractures are induced in unconventional reservoirs in order to extract the oil and gas present in the rock pores (Islam 2014). To induce fractures, water is injected under high pressure in the formation accompanied by proppants, which keep the fractures open after the fracturing process. Then, production begins by recovering the injected water and continues with the production of the oil and/or gas located in the pores of the fractured formation. This technique is employed worldwide and, particularly in Argentina, it is applied to the Vaca Muerta Formation, which is the largest productive unconventional reservoir in the country, presenting a large volume of hydrocarbons in different phases (Askenazi *et al.* 2013).

Seismic waves are sensitive to the presence, orientation and properties of fractures in rocks. For this reason, seismic methods are employed to characterize fractures in subsurface. Seismic waves that propagate through a fractured rock are affected by several physical process which might induce attenuation and velocity dispersion. Some examples are scattering, fluid pressure diffusion (FPD), viscous drag, and inelastic attenuation associated with the solid matrix. Depending on the relation between the wavelength and the scale of the fracture network, one of these processes can be predominant. In a fluid saturated rock, when the wavelength is much larger than the fracture, FPD prevails (White *et al.* 1975; Pride *et al.* 2004; Müller *et al.* 2010). In this sense, the passing wave heterogeneously deforms the rock and, due to the compressibility contrast between the stiff rock matrix and the compliant fractures, induces fluid pressure gradients. Moreover, fluid pressure gradients can also be induced between fractures having different orientations (Rubino *et al.* 2013). If the time provided by half a period of the passing wave is the minimum amount required by the fluid pressure perturbation to affect the maximum region of the fractured rock, attenuation and velocity dispersion are maximal. The effects of fractures and fluid properties on the seismic response due to FPD has been broadly explored by means of analytical, numerical and experimental studies (Chapman 2003; Carcione *et al.* 2013, Rubino *et al.* 2013, Quintal *et al.* 2014, Barbosa *et al.* 2016). However, rock fracture characterization, considering properties of diverse types of relevant host rocks and realistic fracture geometries, remains a complex and largely unexplored topic in the specific literature.

Digital rock physics (DRP) aims to reproduce experimental laboratory measurements by means of numerical simulations of certain physical process in models derived from high resolution rock images (Arns *et al.* 2005, Saenger *et al.* 2011, Madonna *et al.* 2012, Saxena and Mavko 2016, Sommacal *et al.* 2016). This technique has evolved in response to technology improvements of hardware and software from two-dimensional (2D) microscopy images to three-dimensional (3D) micro-computed tomography images (μ-CT images). However, significant technological resources are still needed to handle models having sizes of a representative elementary volume (REV) and, in addition, having high enough resolution to contain the relevant structural details at the micro-scale (e.g., grain contacts, fracture walls roughness). Even considering such limitations, DRP studies can yield information that help to explain and understand physical process at the micro-scale, such as, FPD (Das *et al.* 2019). For instance, the detailed 3D visualization of physical processes, such as fluid and solid displacements, deformations and stresses, among others, contributes to a precise illustration of where energy is being dissipated in the considered model at different frequencies (Lissa *et al.* 2021a). This represents a substantial advantage over analytical and numerical solutions based on over-simplified models.

In this work, we show, for the first time, a DRP analysis of seismic attenuation and velocity dispersion due to FPD in a model derived from a fractured shale sample from the Vaca Muerta Formation. First, we briefly describe the fracture generation in the rock sample and the imaging processes. Second, we describe the workflow employed to generate the numerical model from the μ-CT images, as well as the mathematical formulation of the numerical solution. Then, we show the frequency-dependent P-wave response of the 3D-model. Finally, we perform a parametric analysis of the seismic response of a fractured shale with regard to saturating fluid, fracture geometry, and hydraulic connectivity.

SAMPLE PREPARATION AND IMAGING

The models considered in this study are derived from the μ-CT images of fractured shale sample of the lower zone of the Vaca Muerta Formation provided by Marco *et al.* (2021). The sample, having a cylindrical shape of 1.5 inches of diameter and 2 inches length, was vertically extracted (i.e., perpendicular to the intrinsic layering of the formation). To generate induced fractures representatives of those obtained with hydraulic fracturing, the sample was mechanically fractured using the direct shear technique in the laboratory of YPF Tecnología S.A. (Y-TEC) using a uniaxial cell. Then, the sample was imaged using a computed tomography (CT) scanner. Figure 1 shows the induced fracture network of the 3D μ-CT image having pixel size of 22.16 microns.

METHODOLOGY

Due to the extremely low permeability of the shales, the background, which embeds the fractures, is assumed to be an elastic solid. For the analyzed process, that is, FPD between fractures at seismic frequencies or higher, this is a fair assumption given that the time provided by half the period of the incident wave is not enough to cause FPD between fracture and background. In addition, in this work we only consider P-waves at vertical incidence which means that the intrinsic vertical transverse isotropy of shales is not affecting the results presented here. The scenario

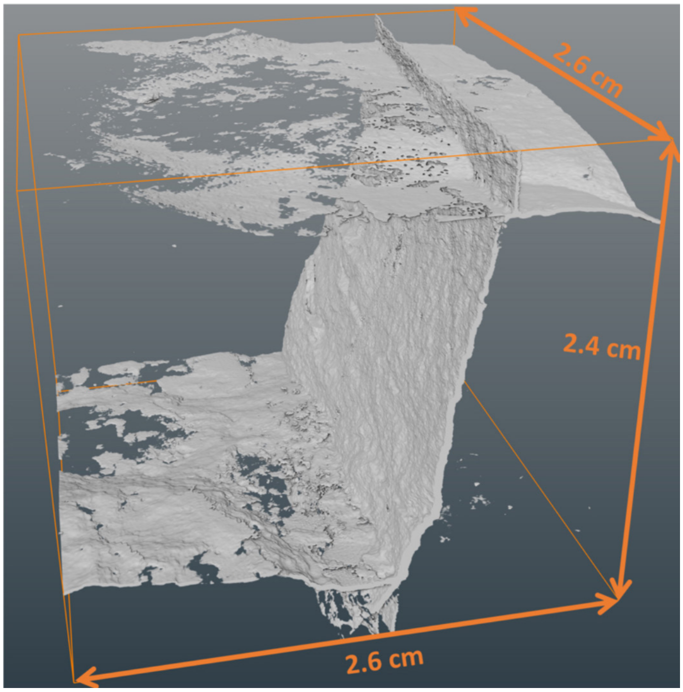

Figure 1. μ-CT image of the fractured shale sample from the Vaca Muerta Formation.

considered in this work is thus representative of the near offset seismic response of compressional waves propagating in a shale formation containing a fully saturated fracture network.

Mathematical formulation

In this work we focus on the energy dissipation of a compressional wave at vertical incidence due to FPD between fluid saturated fractures having different orientations. We follow the quasi-static approach proposed by Quintal *et al.* (2016, 2019) that assumes an elastic background described by Hooke's law embedding fractures which are fully filled with a compressible viscous fluid whose laminar flow is described by the linearized Navier-Stokes equations. This coupled process is mathematically expressed with the conservation of momentum, neglecting acceleration terms,

$$\nabla \cdot \boldsymbol{\sigma} = 0, \tag{1}$$

where $\boldsymbol{\sigma}$ is the total stress tensor, and a generalized constitutive equation in the frequency domain,

$$\sigma_{kl} = 2\mu\epsilon_{kl} + \lambda e\delta_{kl} + 2i\omega\eta\epsilon_{kl} - \frac{2}{3}i\omega\eta e\delta_{kl}, \tag{2}$$

where ϵ_{kl} are the components of the strain tensor, e is the cubical dilatation given by the trace of the strain tensor, δ_{kl} is the Kronecker delta, $\lambda = K - \frac{2}{3}\mu$ is the Lamé parameter written in terms of the bulk (K) and shear (μ) moduli, η is the fluid viscosity, ω is the angular frequency, and i is the imaginary unit.

Eq. 2 is valid for the whole model since in the elastic background is reduced to Hooke's law, by setting the shear viscosity to zero. Conversely, inside the fluid filled fractures, where the shear modulus is zero, it yields

$$\sigma_{kl} = Ke\delta_{kl} + 2i\omega\eta\epsilon_{kl} - \frac{2}{3}i\omega\eta e\delta_{kl}. \quad (3)$$

The combination of Eqs. 1 and 3 yields the quasi-static, linearized Navier-Stokes equations.

Numerical models

We created the numerical models from the μ-CT images (Figure 1) following the methodology presented by Lissa *et al.* (2021a). It consists on denoising, segmenting and meshing the fracture walls of the images using the commercial software Avizo. Then, we create the 3D numerical models using the commercial software COMSOL Multiphysics by extending the mesh from the fracture walls to a volumetric mesh comprising the whole model.

Figure 2a shows the 3D-model employed in this analysis. The fractures depicted in color blue are considered to be fully filled with glycerin, whose properties are summarized in Table 1. Given that the viscosity of glycerin is higher than that of oil and water, it is usually employed in laboratory measurements on saturated rocks to shift the attenuation curve down to the operative frequency range of the laboratory machines. Here, we use glycerin to study attenuation due to FPD between fractures at a frequency range valid for our numerical solution. The background presented in grey is assumed to be an elastic solid (Table 1).

Properties	Bulk modulus K [GPa]	Shear modulus μ [GPa]	Viscosity η [Pa·s]
Solid	27.36	11.12	0
Gas	0.012	0	0.00015
Water	2.25	0	0.001
Oil	1.1	0	0.01
Glycerin	4.35	0	1

Table 1. Material properties of the models.

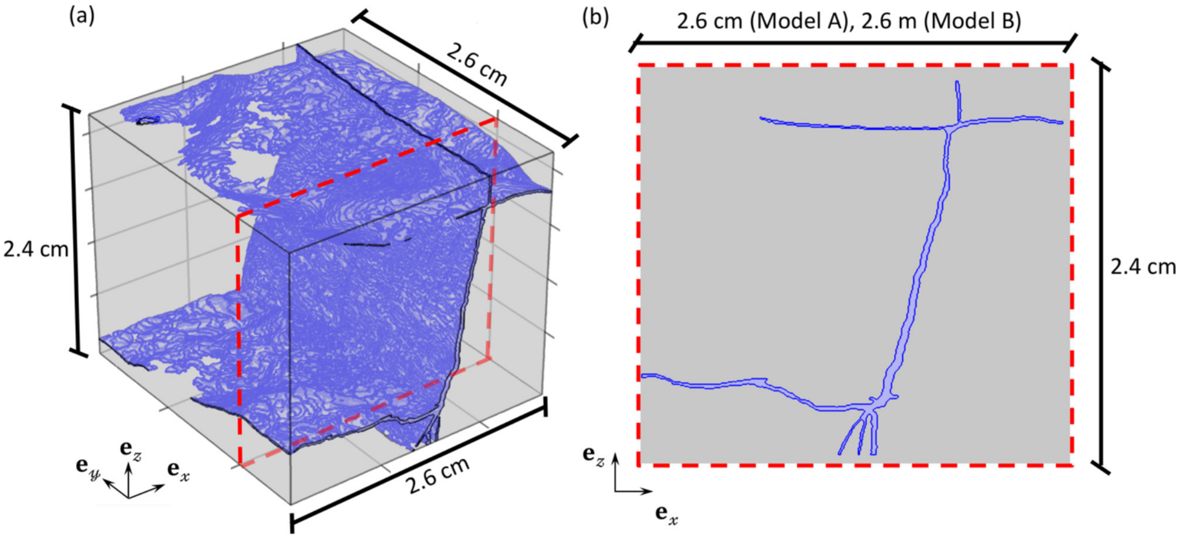

Figure 2. (a) The 3D numerical model and two (b) 2D numerical models. The 2D models (b) have the same height but different widths: Model A has 2.6 cm and Model B has 2.6 m.

For the analyzed physics, reducing the viscosity of the fluid (to study oil, water, or gas saturation effects) shifts the attenuation curve toward higher frequencies than those valid for our numerical solution. In addition, increasing the length of the fractures to study such effect on the seismic response is limited by our hardware capacity due to the extremely high number of elements in the mesh of the 3D numerical model. For these reasons, we derived a 2D model consisting of a slice of the 3D model (Figure 2b).

Due to its low permeability, the shale formation is hydraulically fractured to allow the hydrocarbon extraction. Moreover, sandstone grains or similar materials, usually referred to as proppant, are introduced in the formation to maintain the fractures opened. The fracture aperture in our models is in the range of the diameter of the usually employed proppant (that is 400 microns approximately). However, the fracture length (~1.3 cm) of Model A (Figure 2b) is much shorter than those of the fractures induced in the formation. Aiming to emulate the seismic response of reservoir-scale fractures, we changed the aspect ratio of the sample by extending the model in the horizontal direction. As a result, we increased the quasi-horizontal fracture lengths from 1.3 centimeters to 1.3 meters. This model elongated in the x-direction is called Model B (Figure 2b).

Numerical solution

We solve Eqs. 1 and 2 in the frequency domain using a direct solver from COMSOL Multiphysics based on the finite element method. To study the seismic response in terms of the P-wave modulus dispersion and attenuation, we emulate the deformation caused by a passing compressional wave applying a uniform oscillatory displacement on the top boundary of the model (Quintal *et al.* 2016, 2019). We employ periodic boundary condition to appropriately calculate the P-wave response of a medium that can be described by a periodic repetition of the considered model. Finally, we calculate the effective complex P-wave modulus (H) and the corresponding seismic attenuation (Q_H^{-1}), representative of an equivalent viscoelastic medium, as (Lakes 2009; Jänicke *et al.* 2015):

$$H = \frac{<\sigma_{zz}(\omega)>}{<\epsilon_{zz}(\omega)>}, \tag{4}$$

$$Q_H^{-1} = \frac{<Im\{H(\omega)\}>}{<Re\{H(\omega)\}>}, \tag{5}$$

where σ_{zz} and ϵ_{zz} are the vertical components of the stress and strain tensors, respectively, the symbol $<\cdot>$ denotes volumetric averages, and Re and Im denote the real and imaginary parts, respectively. In this work, we analyze the real part of the P-wave modulus which is representative of the wave velocity behavior in terms of the related viscoelastic effects.

RESULTS

First, we present the seismic response of the 3D numerical model saturated with glycerin. Then, we show the response of a 2D model created from a slice of the 3D model. We study the seismic response of 2D models having different fracture lengths and saturating fluids. Finally, we explore the sensitivity of the seismic response to the connectivity of the fractures.

3D model

Figure 3a shows the real part of the P-wave modulus dispersion and attenuation at vertical incidence for the 3D model saturated with glycerin due to FPD between fractures. The model exhibits P-wave attenuation, and the corresponding velocity dispersion, higher than the minimum magnitudes which can be measured with laboratory experiments (~10^{-3}), at frequencies higher than 10^3 Hz. The attenuation peak due to FPD occurs at 10^5 Hz. Figure 3b shows the fluid pressure inside the fractures normalized with respect to the maximum at 10^5 Hz. It can be observed that the fractures oriented perpendicular to the z-direction, that of maximal deformation produced by a P-wave travelling vertically, present the highest fluid pressure. On the other hand, the fracture vertically oriented remains with the lowest fluid pressure. The fact that those fractures are hydraulically connected allows for FPD between them. At frequencies lower than 10^3 Hz the fluid has much more time than that required to equilibrate the fluid pressure and, thus, attenuation is minimal. Moreover, the stiffening effect of the fluid in the fractures is also minimal, resulting in the lowest P-wave modulus. This is known as the low frequency or relaxed limit.

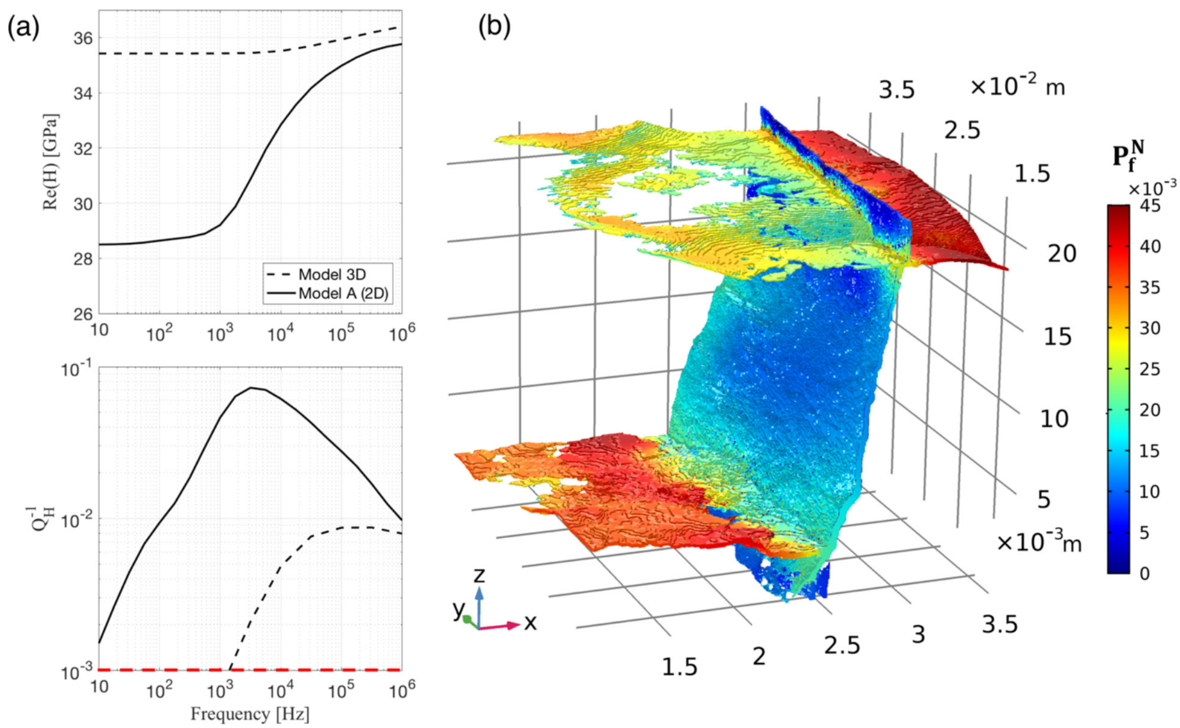

Figure 3. (a) P-wave modulus (H) and attenuation ($1/Q_H$) for a compressional wave at vertical incidence (z-direction) as functions of frequency for the 3D model and the 2D model named Model A. Red dashed line is an estimated minimum attenuation magnitude that can be measured in laboratory experiments. (b) Fluid pressure inside the fractures of the 3D model is shown, normalized with respect to its maximum value, at 10^5 Hz.

2D models

In this section, we first compare the seismic response of our 3D model and 2D model A, which is a slice of the 3D model. Afterwards, we perform a parametric analysis of the saturating fluid, as well as, fracture geometry and connectivity effects on the seismic response of 2D model.

The characteristic frequency f_c (at which the attenuation peak occurs) can be approximated (e.g., Gurevich *et al.* 2010) as

$$f_c \sim \frac{K^s}{\eta}\alpha^3, \tag{6}$$

where K^s is the effective bulk modulus of the fractured sample, $\alpha = {}^{h}/_{L}$ the aspect ratio of the fracture, h and L are the aperture and length of the fracture. The attenuation peak of Model A saturated with glycerin (Figure 3) occurs at lower frequencies (10^3-10^4 Hz), than those obtained for the 3D model (10^5 Hz). The reasons behind this difference can be the change in the fracture length (i.e., L), porosity, and contact areas of the fractures (affecting K^s). For example, the fracture length in the y-direction is finite for the 3D model, but infinite for the 2D model. The same reasons are responsible of the change in the attenuation magnitude and P-wave modulus dispersion. In the following, we perform a parametric analysis using 2D models, as the corresponding analysis in a 3D scenario is not possible due to hardware constrains. Nevertheless, we remark that our analysis remains valid for 3D model expecting a decrease in attenuation and a shift in frequency similar to those showed in Figure 3a.

Figures 4a and 4b shows the P-wave modulus dispersion and attenuation at vertical incidence for Models A and B (Figure 2), and for different fluids saturating the fractures. Due to the decrease of the fluid viscosity, the f_c of Model A saturated with oil is shifted to higher frequencies with respect to that observed for glycerin saturation (as predicted by Eq. 6). In addition, the P-wave modulus of the model saturated with oil is ~10% lower than that saturated with glycerin due to the decrease of the fluid bulk modulus.

Figures 4a and 4b also shows the P-wave modulus and attenuation of Model B saturated with oil and water. The effects of the fracture length (L) on the seismic response can be understood by comparing the solid and dashed green curves. While both models are saturated with oil, the horizontal fractures of Model B are 3 orders of magnitudes larger than those of Model A. It is interesting to note that Model B, having fracture apertures and lengths likely to prevail in a fractured shale formation in field conditions, exhibits significant attenuation in the seismic frequency range [1-100] Hz. In addition, Model B shows a different response when it is saturated with water. In the later scenario, the attenuation occurs at higher frequencies and the P-wave modulus is significantly (~25%) higher than those of the same model saturated with oil. These results highlight the sensitivity of the seismic response to the saturating fluids.

Figure 4 also depicts the saturating fluid (c,d) and fracture length (e,f) effects on the seismic response due to FPD between fractures at 10 Hz (seismic frequency) and 30 kHz (sonic frequency). The P-wave modulus exhibits a decreasing tendency at both frequencies due to the decrease of the saturating fluid bulk modulus (c). On the other hand, the attenuation magnitude changes in the opposite direction at both considered frequencies when changing the saturating fluid (d). For the considered models, the P-wave response is more sensitive to the fracture length at sonic than at seismic frequencies (e). In this sense, a clear increase of the P-wave modulus as function of the fracture length can be observed at 30 kHz. Moreover, the attenuation magnitudes are higher at sonic than at seismic frequencies (f). However, for the considered models, this seismic property is not sensitive to the fracture length.

Finally, we explore the fracture connectivity effects on the seismic response due to FPD. For that, we add small contact areas between the fracture walls closing the fracture. These contact areas are located in the three quasi-horizontal fractures just before they connect with the quasi-vertical fracture. Figures 5a and 5d shows the P-wave modulus and attenuation at vertical incidence for Model B saturated with oil having connected and unconnected fractures. Attenuation and dispersion are drastically reduced when the fractures are unconnected. This demonstrates that the observed attenuation of Model B was mainly due to FPD between connected fractures.

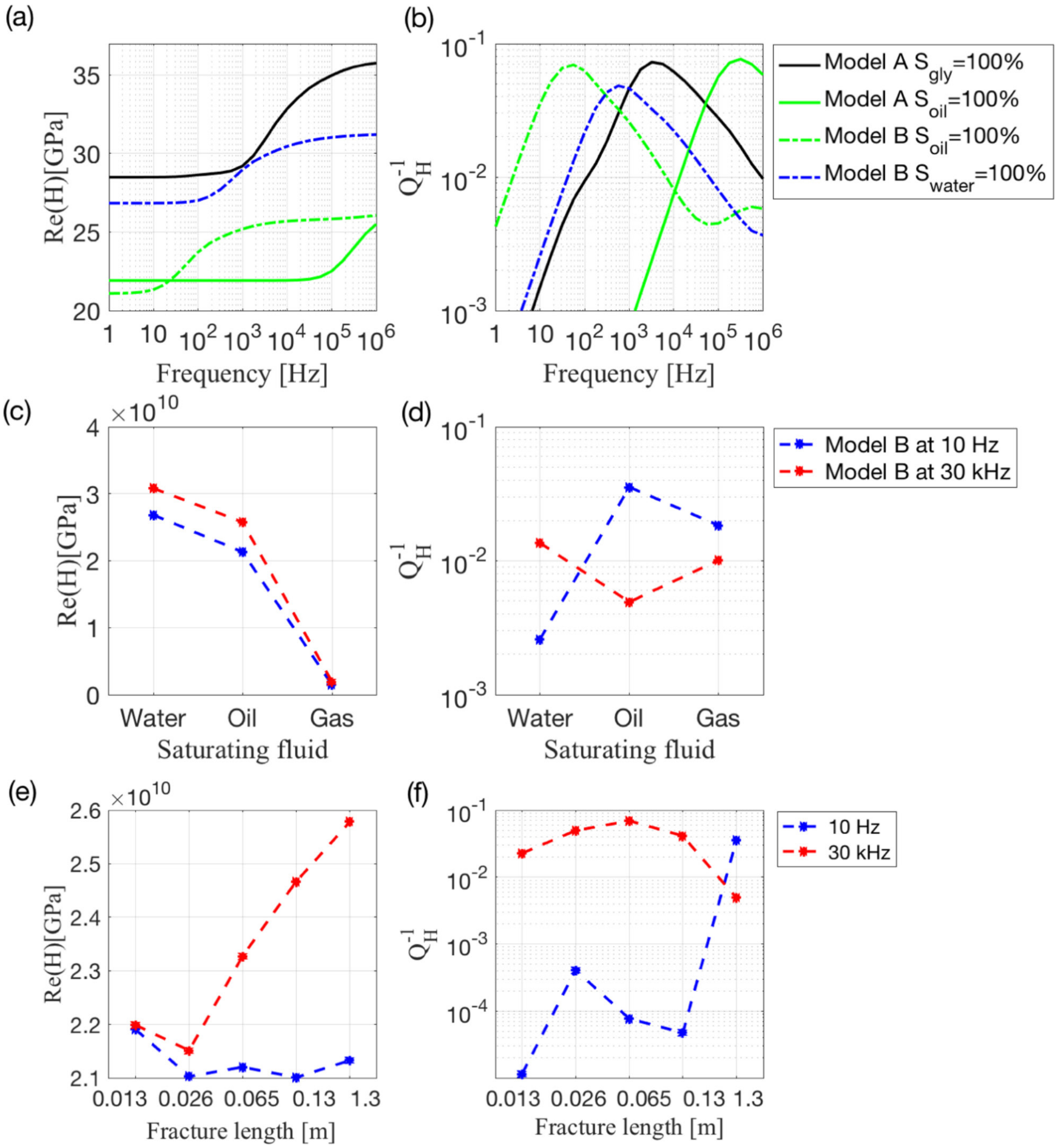

Figure 4. (a) P-wave modulus (H) and (b) attenuation ($1/Q_H$) for a compressional wave at vertical incidence (z-direction) considering the 2D models fully saturated with different fluids as functions of frequency (a,b), and model B at 10 Hz and 30 kHz as function of the saturating fluid (c,d) and, as function of the horizontal fracture length (e,f).

Nevertheless, important seismic attenuation prevails for the unconnected fracture case. To better explain these observations, we plot the fluid pressure P_f^N and the energy dissipation rate D at 100 Hz ($\sim f_c$). Seismic energy is dissipated inside the viscous fluid due to FPD as a response to the wave induced fluid pressure gradients. As an example of that, the excess of attenuation observed at 100 Hz for the connected fracture case (Figure 5d) can be explained with the higher dissipation

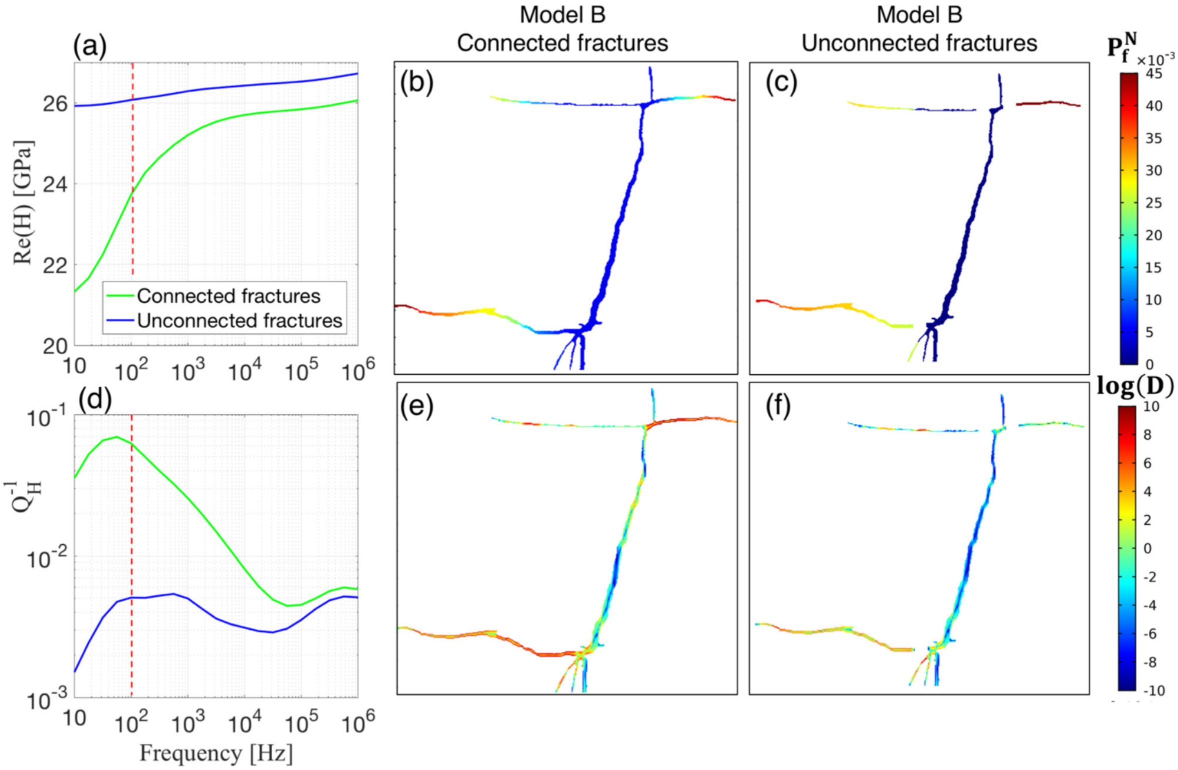

Figure 5. (a) P-wave modulus (H) and (d) attenuation ($1/Q_H$) for a compressional wave at vertical incidence (z-direction) as functions of frequency for Model B fully saturated with oil and having connected and unconnected fractures. Normalized fluid pressure P_f^N (b,c) and energy dissipation rate D (e,f) are shown at 100 Hz (red dashed line).

rate occurring inside the quasi-horizontal fracture located in the upper right side of the model (Figure 5e). While fluid pressure is partially relaxed due to FPD thanks to the connection between fractures for the fracture connected case (Figure 5b), fluid pressure is maximal in the fracture unconnected case (Figure 5c) due to the lack of time to relax during half a period of the P-wave at the analyzed frequency.

Discussion

It is interesting to note that, for Model B saturated with oil and having the fractures disconnected, we still observe significant attenuation (Figure 5a). This occurs because the passing wave generates fluid pressure gradients inside a single fracture due to its curvature as shown by Lissa *et al.* (2021b). Therefore, given that the permeability of fractures is partially controlled by the fracture curvature, seismic methods can be potentially used to infer fracture permeability. Here, we show that such sensitivity of the seismic response to the curvature of fractures, considering geometries that are likely to exist in an oil-saturated shale formation, might occur at the seismic frequency range. Moreover, this effect is observed here for P-wave at normal incidence which is a scenario commonly found in experimental data. Nevertheless, future analyses should be performed to explore the response of the models presented here at variable incidence angles.

For the analyzed models, the attenuation magnitudes at seismic frequencies significantly increased as function of the fracture length (Figure 4f). Attenuation values drastically became higher than 10^{-2} for fracture length larger than 1 meter. This points to the fact that a seismic monitoring survey can potentially provide information about fracture growth during hydraulic fracturing processes.

CONCLUSIONS

In this work, we numerically studied the seismic response in terms of the P-wave modulus dispersion and attenuation due to FPD between hydraulically connected fractures. Following a novel DRP workflow, the numerical models are derived from μ-CT images of a fractured shale sample of the Vaca Muerta formation.

The 3D model saturated with glycerin exhibited significant seismic attenuation due to FPD, which was explained by showing the fluid pressure distribution inside the fractures. Then, we used 2D numerical models to perform a parametric analysis of the fluid properties saturating the fractures, as well as, of the fracture length. We showed that significant seismic attenuation and velocity dispersion can occur at seismic frequencies for fractures having apertures and length which are similar to those expected to prevail in shale formations. In addition, we confirmed the sensitivity of the seismic response to the saturating fluid and to the fracture length. Finally, we showed that P-wave attenuation and dispersion are reduced when fractures are disconnected.

Our results point out the capability of seismic methods to provide valuable information regarding fracture geometry and connectivity, as well as, on the properties of the saturating fluid.

ACKNOWLEDGEMENTS

We gratefully thank YTEC for providing the μ-CT images of a fractured shale sample of Vaca Muerta formation to perform this analysis. We also thank the University of Lausanne for providing the software and hardware used in this work. SL acknowledges the research founding received from the FCAGLP through the Retención de RRHH program. This project has received funding from the European Union’s HORIZON 2020 research and innovation programme under the Marie Skłodowska-Curie grant agreement No. 101007851 (DISCO2 STORE).

REFERENCES

Aguilera, Roberto F., Ripple, Ronald D., and Aguilera, Roberto, 2014, Link between endowments, economics and environment in conventional and unconventional gas reservoirs, Fuel, 126, 224-238, ISSN 0016-2361.

Arns, C., F. Bauget, A. Limaye, A. Sakellariou, T. Senden, A. Sheppard, R. Sok, V. Pinczewski, S. Bakke, and L. I. Berge, 2005, Pore scale characterization of carbonates using X-ray microtomography: SPE Journal, 10, 475-484.

Askenazi, A., Biscayart, P., Cáneva, M., Montenegro, S., & Moreno, M. (2013). Analogía entre la Formación Vaca Muerta y shale gas/oil plays de EEUU. Society of Petroleum Engeneers (SPE).

Barbosa, N. D., Rubino, J. G., Caspari, E., Milani, M., and Holliger, K., 2016, Fluid pressure diffusion effects on the seismic reflectivity of a single fracture, J. Acoust. Soc. Am., 140, 2554-2570.

Carcione, J. M., Gurevich, B., Santos J. E., and Picotti, S., 2013, Angular and frequency-dependent wave velocity and attenuation in fractured porous media, Pure Appl. Geophys., 170, 1673-1683.

Chapman, M., 2003, Frequency-dependent anisotropy due to meso-scale fractures in the presence of equant porosity, Geophys. Prospec., 51, 369–379.

Das, V., T. Mukerji, and G. Mavko, 2019, Numerical simulation of coupled fluid-solid interaction at the pore scale: A digital rock-physics technology: Geophysics, 84, no. 4, WA71-WA81.

Gurevich, B., D. Makarynska, O. B. de Paula, and M. Pervukhina, 2010, A simple model for squirt-flow dispersion and attenuation in fluid-saturated granular rocks, Geophysics, 75(6), N109–N120.

Islam, M. R.,2014, Unconventional gas reservoirs: evaluation, appraisal, and development, Elsevier, ISBN 9780128003909.

Jänicke, R., B. Quintal, and H. Steeb, 2015, Numerical homogenization of mesoscopic loss in poroelastic media: European Journal of Mechanics, A, Solids, 49, 382-395.

Lakes, R., 2009, Viscoelastic materials: Cambridge University Press.

Lissa, S., Ruf, M., Steeb, H., and Quintal, B., 2021a, Digital rock physics applied to squirt flow, Geophysics, 86(4), MR235-MR245.

Lissa, S., Barbosa, N. D., and Quintal, B., 2021b. Fluid pressure diffusion in fractured media: The role played by the geometry of real fractures, Journal of Geophysical Research: Solid Earth, 126, e2021JB022233.

Madonna, C., B. S. Almqvist, and E. H. Saenger, 2012, Digital rock physics: Numerical prediction of pressure-dependent ultrasonic velocities using micro-CT imaging: Geophysical Journal International, 189, 1475-1482.

Marco, S., Sanchez, M., Hyrb, D., Vitolo, M., Fernández Badessich, M., 2021, Efecto de histéresis con degradación sobre la conductividad de fracturas inducidas en la formación Vaca Muerta, 10º Congreso de Exploración y Desarrollo de Hidrocarburos.

Müller, T. M., Gurevich, B., and Lebedev, M., 2010, Seismic wave attenuation and dispersion resulting from wave-induced flow in porous rocks - a review, Geophysics, 75, 147-163.

Pride, S. R., Berryman, J. G., & Harris, J. M., 2004, Seismic attenuation due to wave-induced flow. Journal of Geophysical Research, 109, B01201.

Quintal, B., E. Caspari, K. Holliger, and H. Steeb, 2019, Numerically quantifying energy loss caused by squirt flow: Geophysical Prospecting, 67, 2196-2212.

Quintal, B., Jänicke, R., Rubino, J. G., Steeb, H., and Holliger, K., 2014, Sensitivity of S-wave attenuation to the connectivity of fractures in fluid-saturated rocks, Geophysics, 79, 15-24.

Quintal, B., J. G. Rubino, E. Caspari, and K. Holliger, 2016, A simple hydromechanical approach for simulating squirt-type flow: Geophysics, 81, no. 4, D335-D344.

Rubino, J. G., Guarracino, L., Müller, T. M., and Holliger, K., 2013, Do seismic waves sense fracture connectivity?, Geophys. Res. Lett., 40, 692-696.

Saenger, E. H., F. Enzmann, Y. Keehm, and H. Steeb, 2011, Digital rock physics: Effect of fluid viscosity on effective elastic properties: Journal of Applied Geophysics, 74, 236-241.

Saxena, N., and G. Mavko, 2016, Estimating elastic moduli of rocks from thin sections: Digital rock study of 3D properties from 2D images: Computers & Geosciences, 88, 9-21.

Sommacal, S., Fogden, A., Young, B., Noel, W., Arena, A., Salazar, L., Gerwig, T., Cheng, Q., Kingston, A., Marchal, D., Pérez Mazas, A., Naides, C., Kohler, G., and Cagnolatti, M., 2016, 3D Multiscale Imaging of the Distribution of Pores, Organic Matter and Oil in Place in Vaca Muerta Shale Samples. 10.15530/urtec-2016-2460975.

White, J. E., Mikhaylova, N. G., & Lyakhovitsky, F. M., 1975. Low-frequency seismic waves in fluid-saturated layered rocks. Physics of the Solid Earth, 11, 654-S30.

Zimmerman, R., and Main, I., 2004, Hydromechanical behavior of fractured rocks, InGeo, 89, 363-422.